applied sciences

Article

Wastewater Treatment Using a Combination of *Pumpkin seed* Waste After Extraction of Essential Oils (Bio-Coagulant) and Ferric Chloride (Chemical Coagulant): Optimization and Modeling Using a Box–Behnken Design

Abderrezzaq Benalia [1,2,3], Ouiem Baatache [3], Katr Enada Zerguine [2], Amel Khediri [2], Kerroum Derbal [3,*], Nawal Ferroudj [2], Amel Khalfaoui [4] and Antonio Pizzi [5]

1 Département de Physique Chimie, Ecole Normale Supérieure de Constantine, Nouvelle Ville, Constantine 25000, Algeria; benalia.abderrazzak@ensc.dz
2 École Nationale Biotechnologie de Constantine, Ali Mendjeli Nouvelle Ville, Constantine 25000, Algeria; nadazerguine@gmail.com (K.E.Z.); amelkhediri0405@gmail.com (A.K.); n.ferroudj@ensbiotech.edu.dz (N.F.)
3 Laboratoire de Génie des Procédés pour le Développement Durable et les Produits de Santé (GPDDPS), Département Génie des Procédés, Ecole Nationale Polytechnique de Constantine, Nouvelle Ville, Constantine 25000, Algeria; wiambaatache19@gmail.com
4 Faculté de Génie des Procédés, Université de Constantine 3, Nouvelle Ville, Constantine 25000, Algeria; amel.khalfaoui@univ-constantine3.dz
5 Laboratoire d'Etude et Recherche sur le Matériau Bois (LERMAB), Ecole Nationale Supérieure des Technologies et Industries du Bois (ENSTIB), University of Lorraine, 27 rue Philippe Seguin, 88051 Epinal, France; antonio.pizzi@univ-lorraine.fr
* Correspondence: kerroum.derbal@enp-constantine.dz; Tel.: +213-554687385

Abstract: The wastewater treatment involves various techniques at different technological levels. Treatment takes place in several stages, of which coagulation and flocculation are the most important. Most suspended solids are indeed eliminated during this stage by the addition of a coagulant. In this research, bio-coagulant was extracted from *pumpkin seed* (PS) waste after extraction of the essential oils, and used with ferric chloride to treat wastewater from the plant of Chalghoum El Aid-Oued El Athmania Mila. In this study, the Box–Behnken design (BBD) with three factors was used to investigate the effect of pH, organic coagulant dosage *Pumpkin seed* extract (PSE), and chemical coagulant dosage ($FeCl_3$) on coagulation–flocculation performance in relation to turbidity, chemical oxygen demand (COD), aromatic organic matter (UV 254), and phosphate. The main characteristics of the raw water were turbidity (250 NTU), COD (640 mg/L), UV 254 (0.893 cm^{-1}), and phosphate (0.115 mg/L). The results obtained were very significant. All the statistical estimators ($R^2 \geq 97\%$ and $p \leq 0.05$) reveal that the models developed are statistically validated for simulating the coagulation–flocculation process. It should be noted that the residual values of turbidity, COD, UV 254, and phosphate after treatment by this process were 0.754 NTU; 190.88 mg/L; 0.0028 cm^{-1}; and 0.0149 mg/L, respectively. In this case, the pH, bio-coagulant dosage, and chemical coagulant dosage values were 4; 17.81 mL/L; and 10 mL/L, respectively. In this study, Fourier-transform infrared spectrometer (FTIR) and scanning electron microscope (SEM) characterization of the bio-coagulant proved the presence of the active functional groups responsible for coagulation, namely carboxyl group.

Keywords: wastewater; recovery; *Pumpkin seed* waste; organic coagulant; chemical coagulant; optimization

check for updates

Academic Editors: Veeriah Jegatheesan, Elena Romanovskaia and Valentin Romanovski

Received: 11 April 2025
Revised: 2 May 2025
Accepted: 8 May 2025
Published: 13 May 2025

Citation: Benalia, A.; Baatache, O.; Zerguine, K.E.; Khediri, A.; Derbal, K.; Ferroudj, N.; Khalfaoui, A.; Pizzi, A. Wastewater Treatment Using a Combination of *Pumpkin seed* Waste After Extraction of Essential Oils (Bio-Coagulant) and Ferric Chloride (Chemical Coagulant): Optimization and Modeling Using a Box–Behnken Design. *Appl. Sci.* **2025**, *15*, 5439. https://doi.org/10.3390/app15105439

1. Introduction

The discharge of wastewater into the ecosystem is a major source of pollution and an aesthetic disturbance to aquatic life [1,2]. This practice also generates a potential risk of bioaccumulation [3]. This can affect humans through the transport of these substances in the food chain. Some pollutants can cause allergies and cancer [4,5], Therefore, these waters need to be treated before being released into the environment, using water treatment methods. Several techniques are available for the treatment of wastewater containing major pollutants such as turbidity, total suspended solids (TSS), chemical oxygen demand (COD), nitrogen, phosphorus, etc., including (i) physical processes such as adsorption on activated carbon, membrane filtration, etc [1,6–8]; (ii) advanced oxidation processes: these involve the addition of oxidizing agents such as chlorine (Cl_2), oxygen (O_2), and hydrogen peroxide (H_2O_2) to the treated solution [1,5,9–11]; (iii) biological processes are mainly used to eliminate biodegradable organic substances present in wastewater. These substances are converted into gases that can escape into the atmosphere, and into biological cell tissues that can be eliminated by decantation [12,13]. Another physicochemical process applied in wastewater treatment plants is coagulation flocculation, which results from the addition of iron- or aluminum-based chemical reagents to aqueous dispersions, in order to assemble the dispersed fine particles into larger aggregates. Coagulation is the process of neutralizing the electrical charges of particles in water, allowing them to come closer together. Flocculation follows coagulation and involves gentle mixing to promote the aggregation of these neutralized particles into larger clusters called flocs, which can then be removed from the water. After flocculation, these new aggregates can be removed by processes such as decantation or filtration. The efficiency of this treatment stage depends on the pH, type, and dosage of coagulant, as well as the nature of the particles and the mineral and organic particles. Currently, the majority of plants worldwide use ferric chloride as a chemical coagulant to minimize pollution load (turbidity, COD, etc.). The high concentration of this coagulant has disadvantages, as (i) the presence of residual iron can lead to significant problems for human health and other such pathologies [14–16]. It is therefore toxic to ecosystems. Iron is also toxic to wildlife. This toxicity generates a number of concerns for bovine calves. (ii) The production of sludge loaded with non-reusable and non-biodegradable iron. This sludge can be a source of environmental problems [17,18].

In recent years, a paradigm shift in the wastewater treatment industry has changed the culture of water operators to embrace and implement sustainability in operations. One practical approach is to replace chemical coagulants such as ferric chloride with "green" products that have lower environmental impact in terms of production, consumption, and secondary waste management. Natural coagulants seem to fit the picture and may be an alternative to conventional inorganic coagulants. It has been generally reported that natural coagulants can be easily obtained from renewable materials, produce smaller quantities of biodegradable sludge (potentially reducing the expense associated with sludge disposal), and are less affected by water pH [19,20].

In this work, we focused on the combination of two types of coagulants: a chemical coagulant ($FeCl_3$) and a natural coagulant derived from *Pumpkin seed* extract (PSE). While most studies on coagulation using ferric chloride for wastewater treatment have employed relatively high concentrations of $FeCl_3$, several authors have reported optimal doses ranging from 30 to 200 mg/L. For instance, Prathna et al. identified an optimal dose of 40 mg/L [21], Poon et al. reported around 30 mg/L [22], and Yogesh and Dabhi found that 200 mg/L was necessary to achieve 76% turbidity and 85% COD removal [23]. One of the main objective of this study is to reduce the dosage of the chemical coagulant ($FeCl_3$) by incorporating a natural coagulant (PSE) in order to achieve an efficient and more environmentally sustainable treatment of wastewater.

To this end, the study was carried out in two main stages. The first stage involved the physicochemical characterization of the PSE bio-coagulant using (FTIR) and (SEM). The second stage focused on the optimization and modeling of the coagulation–flocculation process using response surface methodology (RSM). In this part, the (BBD) was applied to evaluate the influence of three variables: pH, $FeCl_3$ dosage, and PSE dosage on the removal efficiency of turbidity, COD, UV 254 absorbance, and phosphate.

The novelty of this study lies in several aspects. Firstly, it proposes the development of predictive mathematical models that could be directly used in wastewater treatment plants to determine optimal operating conditions without requiring a preliminary laboratory-scale optimization step. Secondly, it contributes to the valorization of agro-industrial waste specifically, *Pumpkin seed* residues after essential oil extraction by reusing them as a functional bio-coagulant. Lastly, the combination of an iron-based chemical coagulant with an organic coagulant offers a dual advantage: the effective purification of contaminated water in accordance with Algerian discharge standards, and the complete recovery of waste within a circular economy approach.

2. Materials and Methods

The diagram below represents the sequences used for this study.

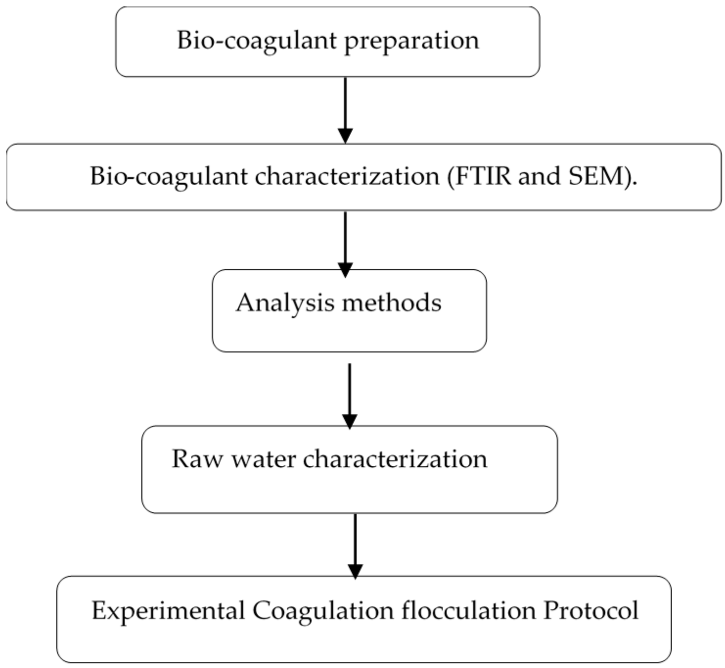

2.1. Preparation of the Bio-Coagulant

Most plant-based coagulants are inaccessible due to their high cost and limited availability in certain regions, which poses challenges for water treatment. The seasonal availability of these materials is also a significant factor. To address this, we chose to utilize *Pumpkin seed* waste, a by-product from the extraction of essential oils, to prepare a low-cost bio-coagulant. The PS bio-coagulant used in this study is derived from this industrial waste, obtained directly after essential oil extraction at a production unit in Dréan, El Tarf, Algeria (36°45′21″ N, 7°44′30″ E). It is composed solely of *Pumpkin seeds* (PS), without any additional components or processing. This material not only offers a cost-effective solution but also contributes to the valorization of waste from essential oil production, an area where the waste is currently underutilized and unrecycled.

A pretreatment of the PS sample was applied, including low-temperature drying to prevent denaturation of the coagulating agents, grinding to reduce the size of the particles, and sieving to obtain the fine, homogeneous powder of the coagulant (d < 0.35 mm) (see Figure 1a).

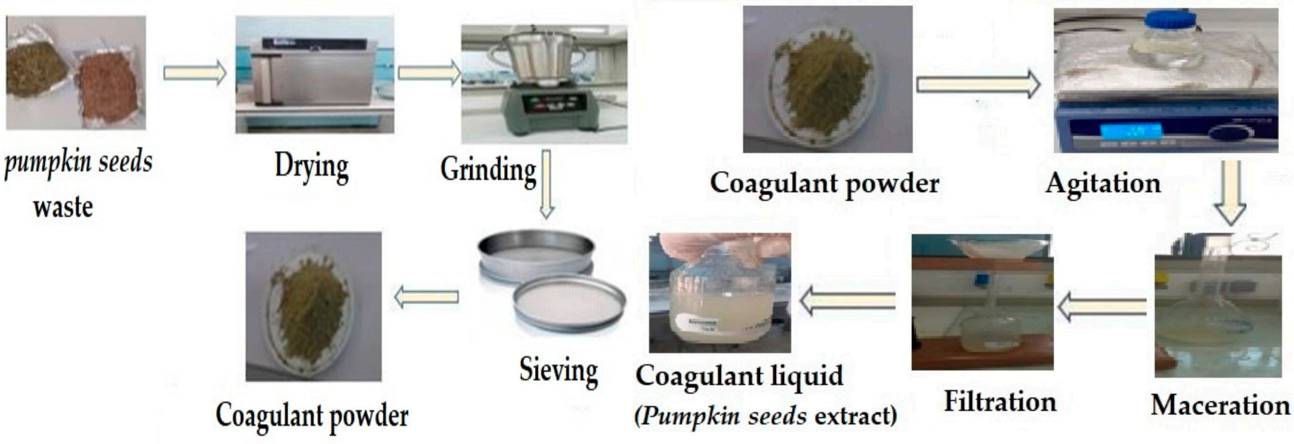

(**a**) (**b**)

Figure 1. Extraction and purification of coagulant agents from *Pumpkin seeds:* (**a**) powdered and (**b**) liquid form (*Pumpkin seed* extract).

The extraction of coagulating agents is a crucial and critical step that can be influenced by various factors that need to be optimized to achieve a higher coagulant yield. Optimization involves pH adjustment, solvent type, solvent concentration (NaCl), and agitation time. Based on the previous analysis, 0.5 g of powdered coagulant was added to 100 mL of NaCl solution (1.17 M) with a pH of 12.045. The mixture was stirred at 700 rpm for 73.63 min. After 30 min of maceration, the supernatant was filtered through standard filter paper (porosity < 8 µm). The filtered solution was used as a bio-coagulant (see Figure 1b) [19].

2.2. Analytical Methods

A portable turbidity meter of the brand HACH and Digital Reactor Block 200 (Jenway model 3540, Camlab, Cambridge, UK) were used to measure the turbidity and the chemical oxygen demand (COD), respectively. The pH, conductivity, and salinity were measured using multi-parameter probe (Jenway model 3540, Camlab, Cambridge, UK). The total alkalinity (TAC), sulfate, chloride, and aromatic organic matter (Abs at 254 nm) were determined by standard titrimetric methods [24]. The infrared spectrum of *Pumpkin* was obtained with a Fourier-transform infrared spectrometer (SHIMADZU Code: HI 98713, Shimadzu, Cluj Napoca, Romania) in the range of 4000–500 cm^{-1}. The scanning electron microscopy (SEM) images of *Pumpkin* were acquired with scanning electron microscope (Hitachi TM3400, Hitachinaka, Japan).

2.3. Raw Wastewater

The coagulation–flocculation process was used as a primary and tertiary process in the treatment chain to improve the quality of raw wastewater and treated wastewater from the Chalghoum El Aid-Oued El Athmania plant, Mila (36°27′1.01″ N; 6°15′51.98″ E). The main characteristics of raw wastewater are reported in Table 1.

Table 1. Raw water characterization.

Parameter	Value	Algerian Standards [25]
Turbidity (NTU)	250	/
COD (mg/L)	640	120
UV 254	0.893	/
Temperature (°C)	24	30
Phosphate (mg/L)	0.115	/
Salinity (mg/L)	5.5	/
Conductivity (mS/cm)	9.15	
pH	8.25	6.5–8.5
Sulfate (mg/L)	2.35	/
TAC (mg/L $CaCO_3$)	100	/
Chloride (mg/L)	4.2	/

2.4. Experimental Coagulation–Flocculation Protocol

Laboratory evaluation of coagulation–flocculation was conducted using a VELP SCIENTIFICA Jar Test apparatus, a standard 4-station rotational device with speeds ranging from 20 to 200 rpm. Tests were performed in 1000 mL beakers following the standard protocol of coagulation–flocculation–sedimentation, after adjusting the solution pH using HCl (1 mol/L) or NaOH (1 mol/L). After settling, the supernatant was sampled, and pollution parameters including COD, turbidity, UV 254, and phosphates were measured.

In this study, the response surface method (RSM) based on Box–Behnken design (BBD) was used as the experimental methodology using Minitab 18 software (Minitab, LLC, State College, PA, USA). The RSM is used to determine optimal ranges based on statistical techniques, and determine whether a process condition leads to an optimal value of a response variable. Through RSM, a quadratic polynomial equation was developed to predict the response as a function of the independent variables involving their interactions. This enables second-order response surfaces to be modeled. The most commonly used designs at this stage are the Box–Behnken design (BBD) and the central composite design (CCD). All these optimization designs were used to obtain and fit experimental data with a polynomial multiple linear regression model to characterize the response surface.

Box and Behnken introduced an alternative type of experimental design for second-order models that allows for the estimation of certain interactions [26]. The BBD has the following properties: (i) it requires three levels for each of the factors; −1, 0 and +1 to ensure the orthogonality condition; (ii) it possess the sequentiality property; (iii) prediction errors are lower than experimental errors. According to Bezerra et al., this model offers greater efficiency and cost effectiveness than other three-level models, namely the central composite design, because it allows for the selection of points in a three-level factorial arrangement [27]. According to the BBD, three factors (k = 3) were taken into account in the coagulation–flocculation performance, namely pH, the organic coagulant dosage (PSE) and a chemical coagulant dosage ($FeCl_3$). This design required 15 experiments with three central points, as mentioned in Table 2, and mathematical models for each response (turbidity, COD, UV 254, and phosphate) were obtained using Equation (1).

$$Y_i = B_0 + \sum_{i=1}^{k} B_i * X_i + \sum_{i=1}^{k} B_{ii} * X_i^2 + \sum_{\substack{i=1 \\ j=2 \\ i \neq j}}^{k} B_{ij} * X_i * X_j + \varepsilon \quad (1)$$

where Y_i is the response variable; K: the number of factors (K = 3); X_i: the parameters studied; β_0: the constant value; and β_i, β_{ii}, β_{ij}: the regression coefficients.

Table 2. Experimental plan with real values.

Standard Run	pH (X_1)	PSE Dosage (mL/L) (X_2)	$FeCl_3$ Dosage (mL/L) (X_3)
4	10	20	5.5
1	4	2	5.5
6	10	11	1
14	7	11	5.5
5	4	11	1
15	7	11	5.5
10	7	20	1
12	7	20	10
2	10	2	5.5
13	7	11	5.5
8	10	11	10
11	7	2	10
7	4	11	10
9	7	2	1
3	4	20	5.5

3. Results and Discussion

3.1. Characterization of Bio-Coagulant

Fourier-transform infrared spectroscopy was used to identify the functional groups in the powdered form of the PS bio-coagulant. Figure 2 shows the obtained results. Several peaks are present, reflecting the presence of various functional groups.

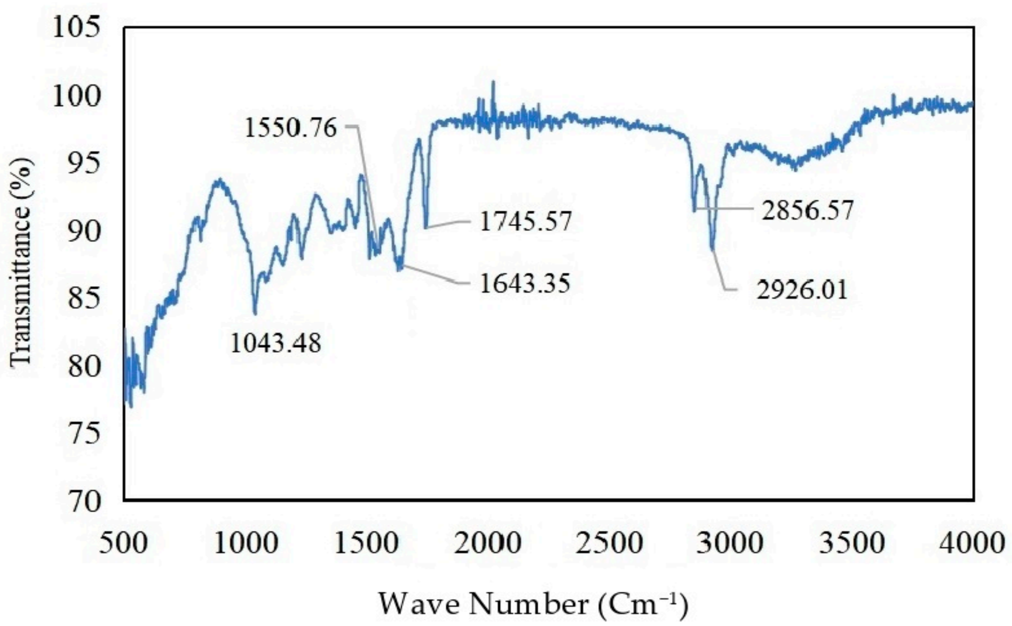

Figure 2. FTIR results for *Pumpkin seed* waste powder form.

At 2856.57 and 2926.01 cm^{-1}, peaks indicate the presence of the C-H group (a single bond between carbon and hydrogen), ester groups (the C=O function) attributed to the band at 1745.57 cm^{-1}, and amide groups associated with proteins assigned to the peak centered at 1643.35 cm^{-1} [28,29]. The presence of the C=C double bonds and polysaccharides (COOH groups) was inferred from the bands at 1550.76 cm^{-1} and 1043.48 cm^{-1}, respectively [30].

The presence of certain functional groups, such as NH- at 1643.35 cm^{-1}, C=O at 1745.57 cm^{-1}, and COOH at 1043.48 cm^{-1}, confirms the presence of various coagulating agents, including polysaccharides, total phenolics, and protein in *Pumpkin seeds*. These functional groups contribute to the efficiency of the coagulation process by providing adsorption sites for suspended and colloidal matter, thereby facilitating the removal of turbidity, COD, phosphate, and UV 254 absorbance [28].

Figure 3 shows the surface morphology of the powdered coagulant, which confirms its heterogeneous nature. This structure facilitates the process of coagulation–flocculation due to the presence of the functional groups in PS, such as amine, amide, protein, and carboxylic acids [31]. Conversely, the presence of fibrous networks may assist in the adsorption and bridging of various pollutants present in the wastewater such as COD, turbidity, aromatic compounds, and phosphate [32].

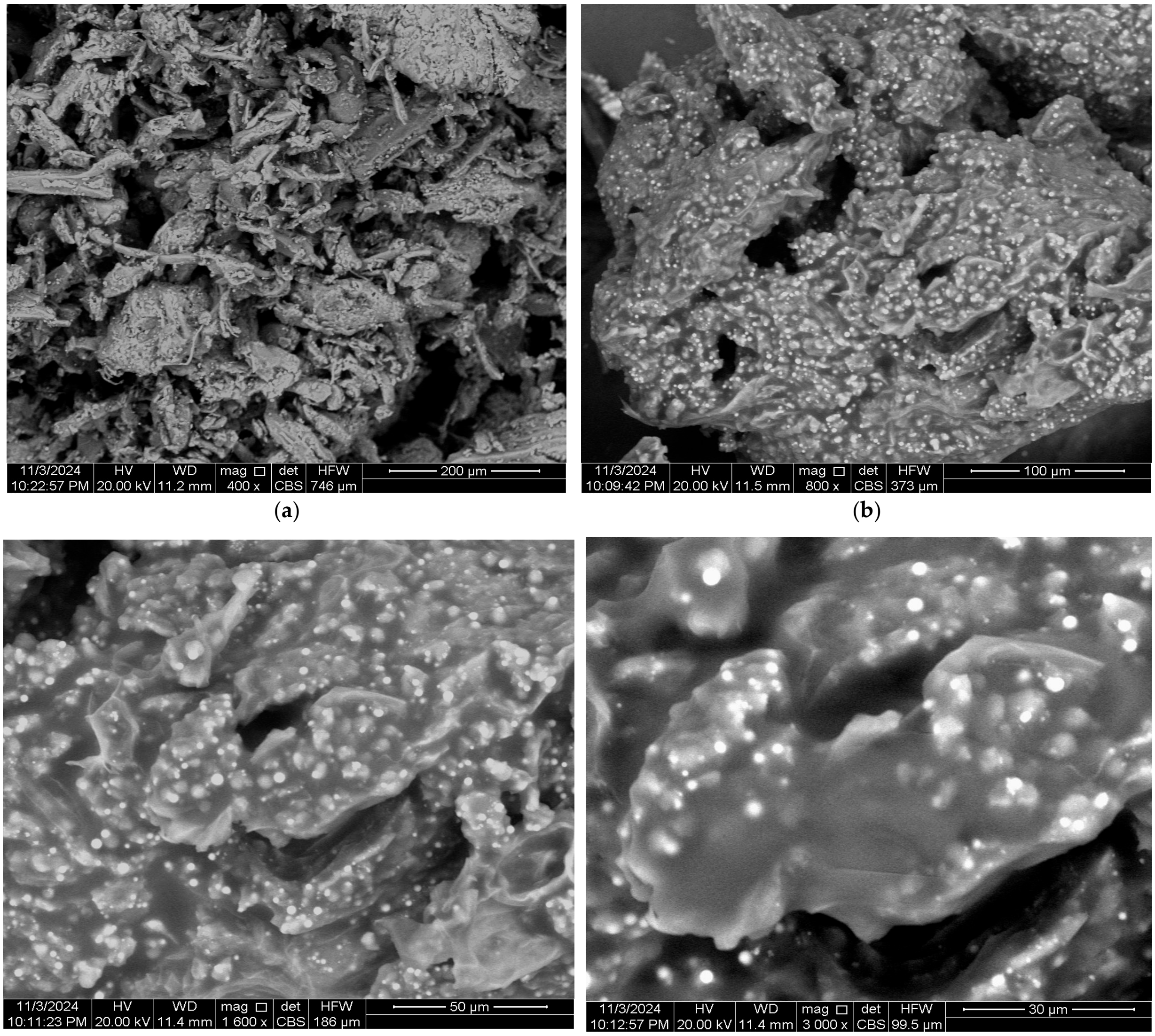

Figure 3. SEM results for *Pumpkin seed* waste powder form (**a**): 200 µm; (**b**): 100; (**c**): 50 µm; and (**d**) 30 µm.

3.2. Optimization and Modeling of Coagulation–Flocculation Process

The complete quadratic regression models for coagulation are given in real form by the following equations:

$$\text{Turbidity (NTU)} = 3.506 - 0.246\,X_1 - 0.1866X_2 - 0.0575\,X_3 + 0.0157\,X_1^2 + 0.00088X_2^2 + 0.00070\,X_3^2 + 0.01889\,X_1X_2 - 0.02426\,X_1X_3 + 0.00648\,X_2X_3 \quad (2)$$

$$\text{COD (mg/L)} = 243.3 + 37.8\,X_1 + 3.29X_2 - 61.36X_3 + 5.185\,X_1^2 + 0.146\,X_2^2 + 2.609\,X_3^2 - 0.463\,X_1X_2 + 7.519X_1X_3 - 0.790X_2X_3 \quad (3)$$

$$\text{UV 254}\ \left(\text{cm}^{-1}\right) = 0.7887 - 0.0843\ X_1 - 0.01248\ X_2 - 0.09190\ X_3 - 0.00084\ X_1^2 - 0.000223\ X_2^2 + 0.000431\ X_3^2 + 0.002713\ X_1X_2 + 0.011037\ X_1X_3 + 0.000556\ X_2X_3 \quad (4)$$

$$\text{Phosphate}\ (\text{mg/L}) = 0.06099 - 0.00911\ X_1 - 0.002158\ X_2 - 0.000573\ X_3 + 0.000518\ X_1^2 + 0.000070\ X_2^2 + 0.000033\ X_3^2 + 0.000093\ X_1X_2 + 0.000076\ X_1X_3 - 0.000049\ X_2X_3 \quad (5)$$

3.3. Effects Graphs

All the investigated operational parameters significantly influence the removal of turbidity, COD, UV 254, and phosphate through coagulation and flocculation processes.

3.3.1. Effect of pH

The coagulation–flocculation process is strongly influenced by the initial pH of the raw wastewater, as it affects the efficiency of particle aggregation and removal [33]. The initial pH of the water sample was 8.25. However, for this study, it was adjusted to 4, 7, and 10 to evaluate the coagulant performance in acidic, neutral, and alkaline conditions.

Figure 4a–d presents the experimental results, demonstrating the influence of pH on the effectiveness of coagulation in removing turbidity, COD, UV 254, and phosphate.

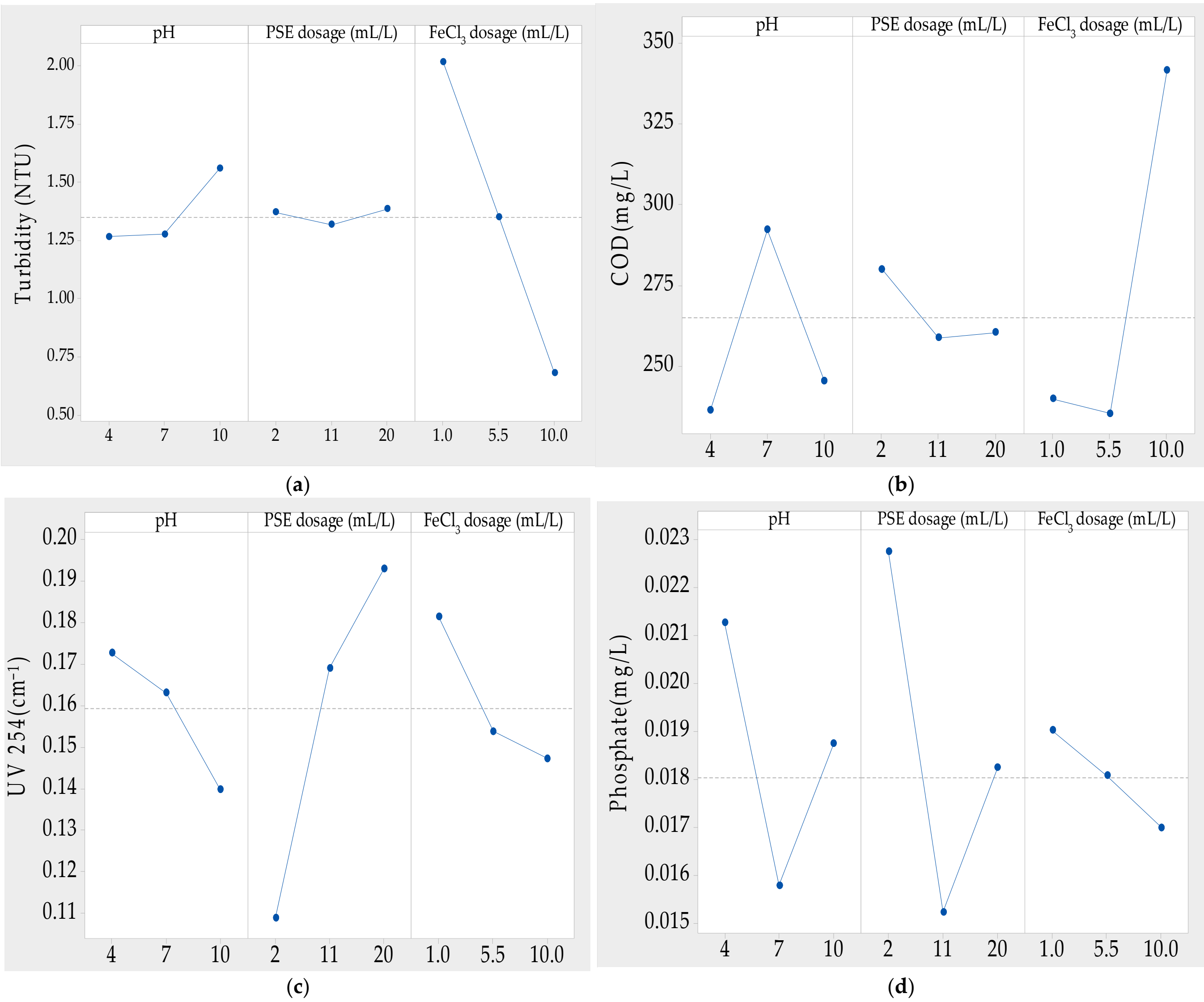

Figure 4. Graphs of the effects of different parameters used in the application of its coagulating agents on raw wastewater (**a**): turbidity; (**b**): COD; (**c**): UV 254; (**d**): phosphate.

For turbidity and phosphate removal, the highest efficiency is achieved at pH 7 (Figure 4a,d). Under acidic conditions, a low pH leads to an excess of H^+ ions, which compete with active compounds in the polymer chain, disrupting the flocculation process by hindering the bridging mechanism. Conversely, in alkaline conditions, an excess of OH^- ions induces a sweeping effect, potentially enhancing turbidity and phosphate removal [34]. Nevertheless, as reported by Desta et al. [35], pollutant removal efficiency improved as pH increased to 9, but further increases led to a decline in removal performance. At pH 3, the acidic environment rendered the process largely ineffective. Moreover, results at pH 7 indicated that the flocs formed by the selected natural coagulant were large and developed quickly, facilitating efficient settling [34,36].

For COD removal, the highest efficiency was observed at pH 4. As shown in Figure 4b, the COD concentration decreased to below 250 mg/L at this pH. However, when the pH increased to 7, COD removal declined significantly, stabilizing at 300 mg/L. A subsequent rise in COD removal was observed at pH 10. The optimal coagulation at pH 4 was attributed to favorable interactions between $FeCl_3$, PSE, and wastewater contaminants. As the pH increased to 7, coagulation efficiency decreased, reducing the removal of dissolved organic matter, which primarily contributed to COD. At this pH, the balance of charged particles led to a stabilization in removal efficiency. Additionally, turbidity removal improved, reaching its peak at pH 7. The increase in pH neutralized the positive charge present at pH 4, enhancing particle agglomeration and flocculation [19,37].

For UV 254, the highest removal efficiency is observed at pH 10, as shown in Figure 4c. The data indicate a negative correlation between UV 254 removal and low pH levels. As the pH increases from 4 to 10, UV 254 removal improves, suggesting a high concentration of aromatic organic matter in the wastewater samples. The reduced UV 254 removal at low pH can be attributed to the protonation of functional groups, which weakens their interaction with organic compounds, preventing effective adsorption onto the coagulant surface.

3.3.2. Effect of *Pumpkin seed* Extract Dose

The removal efficiency of pollutants strongly depends on the coagulant dosage, which can be categorized as insufficient (under-dosage), optimal, or excessive (over-dosage). Optimizing the coagulant dosage is essential for improving wastewater treatment efficiency [28,38], as shown in Figure 4a,b,d. A dose of 2 mL/L of PSE is insufficient to adsorb all pollutants (turbidity, COD, and phosphate removal), leading to incomplete coagulation. Consequently, a higher dosage is required to achieve effective treatment. At 11 mL/L, which represents the optimal dosage, the removal of turbidity, COD, and phosphate is maximized. This is primarily due to the high protein content in PSE, which enhances floc formation through charge neutralization (by interacting with oppositely charged ions) and bridging mechanisms (by forming particle–polymer complexes during adsorption onto polymer chains) [39]. However, exceeding this optimal point, such as with a dose of 20 mL/L, leads to over-dosage. Additionally, the excess coagulant saturates the colloidal surfaces, causing particle restabilization, which hinders floc formation and ultimately reduces treatment efficiency [38].

Figure 4c shows that the residual UV 254 increased with increasing coagulant dosage, indicating that the optimal dosage for achieving the maximum reduction in UV 254 is 2 mL/L. This phenomenon can be attributed to the organic nature of the PSE coagulant used in the study. Its composition imposes a limitation on its effectiveness for this parameter, as excessive doses may introduce additional organic matter into the treated water [40].

3.3.3. Effect of Chemical Coagulant $FeCl_3$

An increase in $FeCl_3$ dosage beyond 10 mL/L led to a rise in turbidity, UV 254, and phosphate removal, as shown in Figure 4a,c,d. However, for COD removal (Figure 4b), the residual COD increased when the $FeCl_3$ dosage exceeded 5.5 mL/L.

At low coagulant doses, the double layer surrounding colloidal particles remained intact, preventing effective aggregation and floc formation. As the coagulant dosage increased, the neutralization of surface charges facilitated the binding of particles, leading to the rapid formation of visible flocs through sweep flocculation or enmeshment in precipitate. However, beyond the optimal dosage, excess $FeCl_3$ resulted in charge reversal and the destabilization of formed flocs, reducing treatment efficiency. At higher dosages, the surplus coagulant introduced excessive positive charges, preventing proper particle aggregation and leading to colloidal restabilization. Consequently, this negatively impacted water quality [41]. Based on the study's findings, the optimal $FeCl_3$ dosage for achieving maximum reduction in turbidity, UV 254, and phosphate is 10 mL/L, whereas for COD removal, the optimal dose is 5.5 mL/L.

3.4. Contour Plots (2D) and Response Surface Plots (3D)

To improve understanding of the impacts of independent variables and their interactions, response surface plots were used. These graphs were designed in both two dimensions (2D) and three dimensions (3D), indicating the relationship between two variables while keeping the third variable at a constant level of zero [19]. They were used to evaluate the optimum zone for each factor.

3.4.1. Turbidity Removal

The interaction between pH and the dosage of PSE significantly influences turbidity removal. As shown in Figure 5a,b, increasing the coagulant dosage while maintaining a lower pH (acidic conditions) results in a reduction in residual turbidity in wastewater, indicating an improvement in turbidity removal efficiency. The improvement in turbidity removal at higher doses of PSE is mainly due to the increased concentration of active compounds [42], which are more effective in acidic conditions (pH = 4). These compounds interact with suspended particles, facilitating floc formation. This effect can be attributed to the positive charges on the protein molecules present in PSE. At pH levels below 4, most proteins carry a positive charge, allowing them to function effectively as cationic coagulant agents [43,44]. This enhances their ability to neutralize negatively charged particles, promoting coagulation and improving wastewater treatment efficiency.

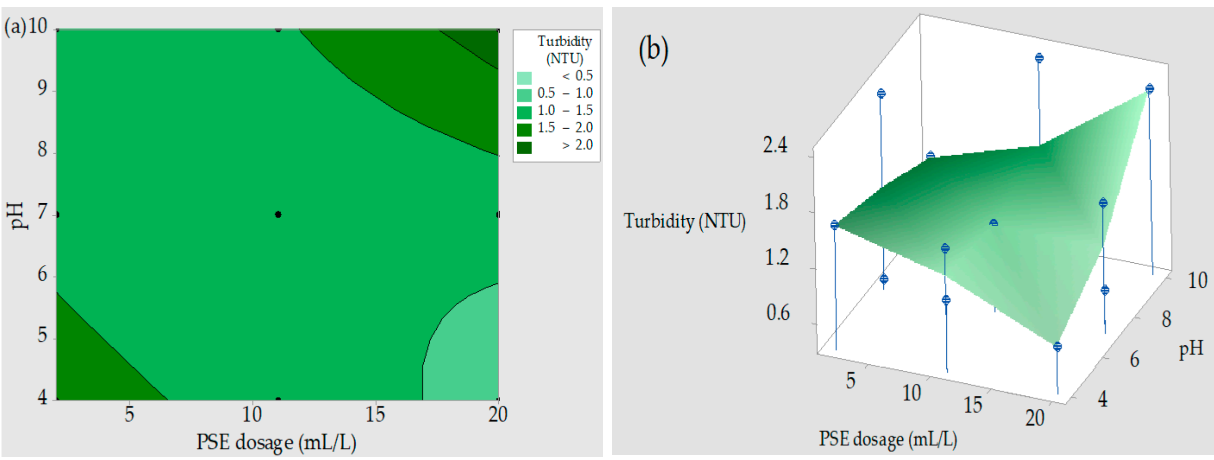

Figure 5. *Cont.*

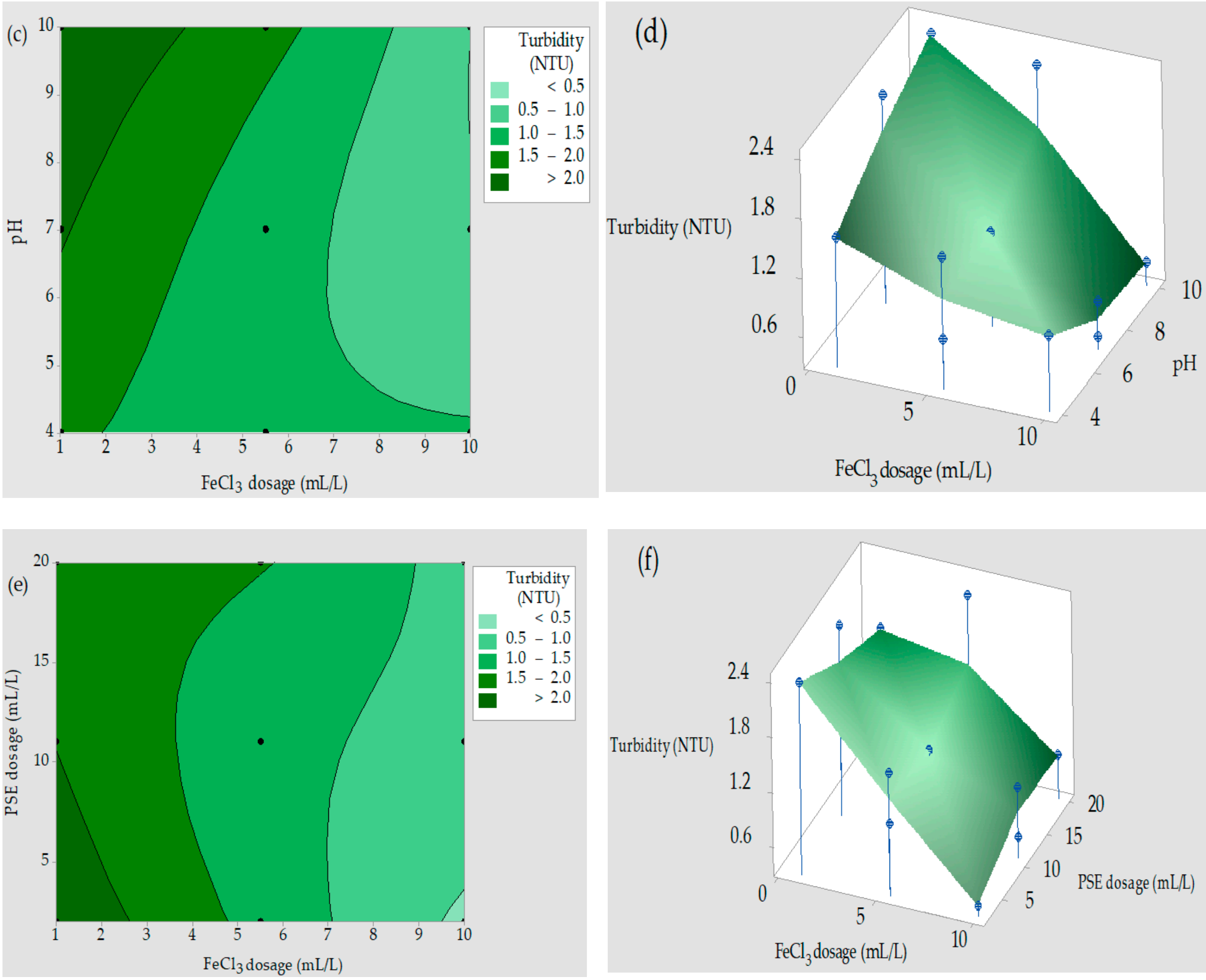

Figure 5. Contour plots and their corresponding surface plots for the turbidity of wastewater as a function of (**a**,**b**) pH and PSE dosage at constant $FeCl_3$ dosage; (**c**,**d**) pH and $FeCl_3$ dosage at constant *Pumpkin* dosage; (**e**,**f**) PSE dosage and $FeCl_3$ dosage at constant pH.

Similarly, Figure 5c,d illustrate the interaction between pH and the chemical coagulant $FeCl_3$. Turbidity removal improves as the $FeCl_3$ dosage increases while maintaining a pH of up to 5. This can be explained by the strong influence of pH on the coagulation activity of chemical coagulants, as pH affects charge neutralization and floc formation. Additionally, Figure 5e,f highlight the combined effect of PSE and $FeCl_3$ on turbidity removal. The data indicate that increasing the dosage of both natural and chemical coagulants leads to a further decrease in residual turbidity. This suggests that both coagulants play a crucial role in destabilizing and attracting suspended solids, thereby enhancing the overall coagulation process.

3.4.2. COD Removal

The increase in wastewater pH up to 9 across all the tried PSE doses contributed to COD removal. As shown in Figure 6a,b, the highest COD reduction was observed at pH 10 with coagulant dosages exceeding 10 mL/L. The effectiveness of PSE in COD removal is attributed to its ability to degrade organic matter, facilitated by its bioactive compounds. The high protein content in *Pumpkin seeds* plays a crucial role in this process, as proteins bind to organic compounds, enhancing their biodegradation by microorganisms, which utilize them as carbon sources through hydrolytic enzymes [45]. However, this activity is highly dependent on pH conditions. Conversely, as shown in Figure 6c,d, the interaction between $FeCl_3$ and pH is stronger than that of the PSE coagulant. The data indicate that the residual COD concentration remained below 150 mg/L. It is important to note that the reduction in COD with $FeCl_3$ is primarily driven by a chelation process, where Fe ions bind to organic matter, promoting coagulation. However, excessive $FeCl_3$ concentrations negatively impact COD removal by reducing the affinity of organic compounds to adsorb onto Fe ions, thereby diminishing treatment efficiency [45].

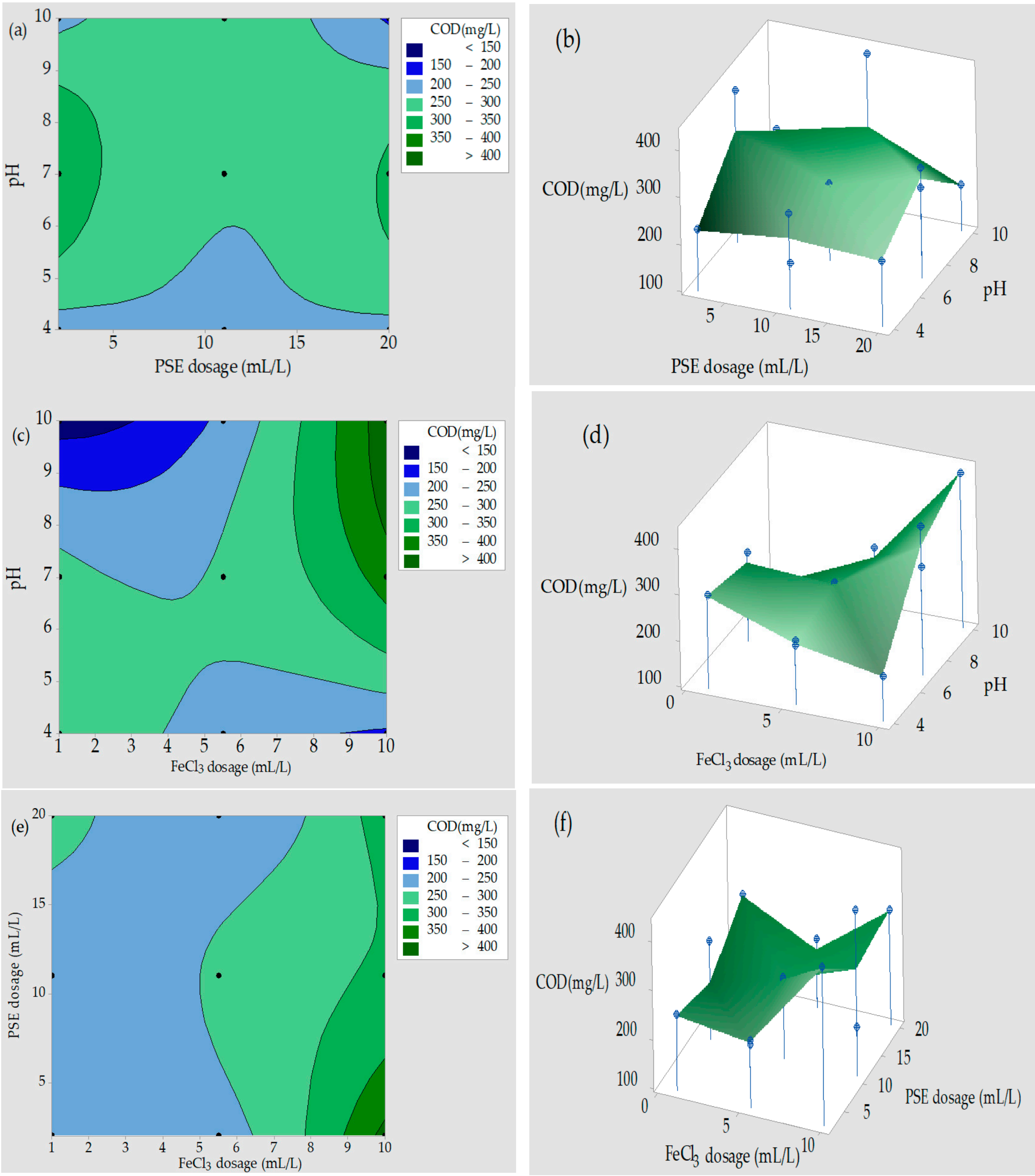

Figure 6. Contour plots and their corresponding surface plots for COD of wastewater as a function of (**a**,**b**) pH and PSE dosage at constant $FeCl_3$ dosage; (**c**,**d**) pH and $FeCl_3$ dosage at constant PSE dosage; (**e**,**f**) PSE dosage and $FeCl_3$ dosage at constant pH.

The impact of the interaction between chemical and natural coagulants is less significant, as indicated in Figure 6e,f, with the maximum reduction in COD achieved within the range of 200 mg/L to 250 mg/L. The limited interaction between chemical and natural coagulants may be due to competition for binding sites or differences in their optimal working conditions. Further investigations are needed to explore potential synergistic effects and to optimize their combined application for enhanced wastewater treatment efficiency.

3.4.3. UV 254 Removal

The interaction between the dose of PSE and pH is shown in Figure 7a,b. It can be observed that when the minimal dose is maintained at neutral and basic pH levels, the removal of UV 254 reaches its maximum. However, at these pH levels, using high doses of PSE in water treatment has the drawback of increasing the organic load in the treated water and removing fewer compounds absorbing at 254 nm compared to other parameters such as COD, turbidity, and phosphate. In combination, pH and dose were statistically significant, as shown in Equation (4).

Figure 7c,d shows that UV 254 removal is maximized at the high pH of 10 (basic) and minimized at a $FeCl_3$ dosage of 1 mL/L. This could be due to the fact that at low pH levels (4 to 7), lower doses of the chemical coagulant are sufficient to initiate charge neutralization and precipitation [46]. Additionally, at the highest $FeCl_3$ dosage (10 mL/L) and the lowest pH (4, acidic), the residual UV 254 is significantly reduced. This may be attributed to charge reversal and restabilization occurring at higher coagulant dosages [46]. Furthermore, the dose of PSE exhibits a positive synergistic effect when combined with pH and the chemical coagulant $FeCl_3$. This is confirmed by the positive terms in the model equation, as seen in Equation (4).

By analyzing the residual values in Figure 7e,f, it can be seen that using a lower dose of PSE in combination with the chemical coagulant $FeCl_3$ (across all studied regions) resulted in a maximum reduction in UV 254 at a neutral pH (7). This behavior is mainly attributed to the fact that the combination of $FeCl_3$ and PSE at a lower dose may create a synergistic effect, enhancing the coagulation process and minimizing the presence of residual organic compounds that absorb UV at 254 nm, thereby leading to a higher UV 254 reduction.

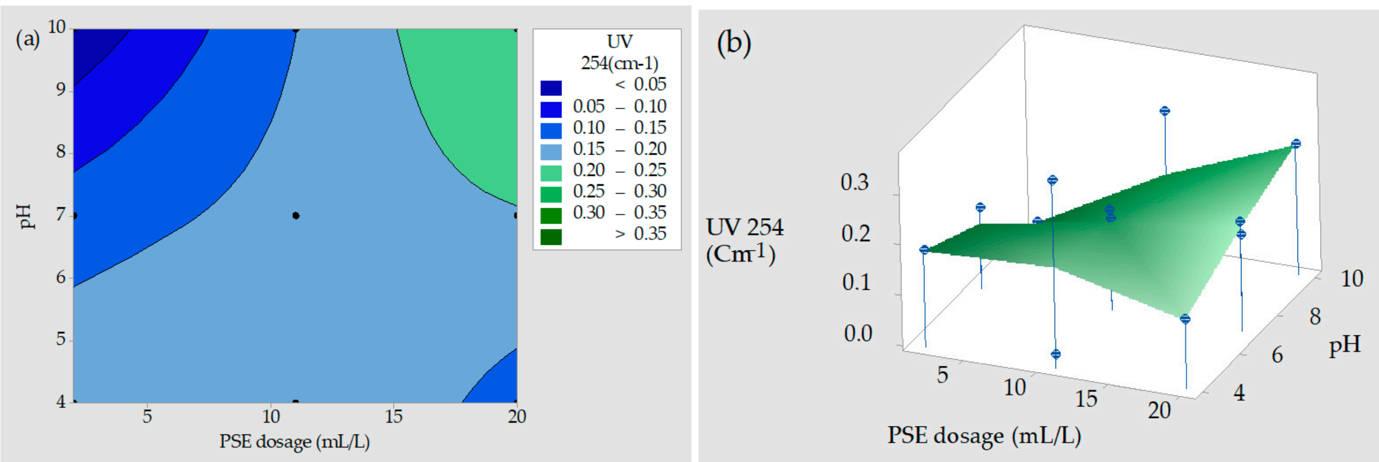

Figure 7. *Cont.*

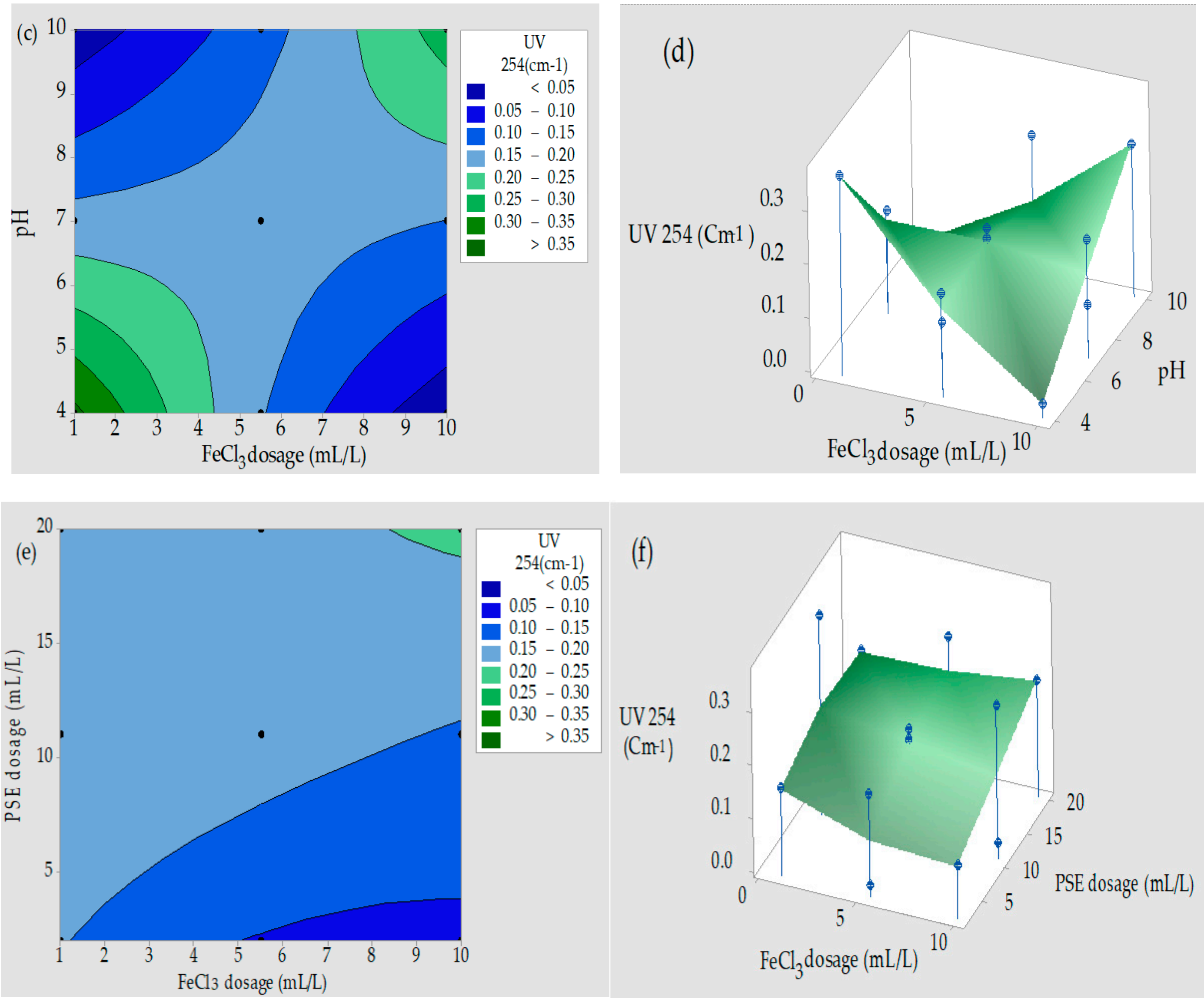

Figure 7. Contour plots and their corresponding surface plots for aromatic matter (UV 254) of wastewater as a function of (**a**,**b**) pH and PSE dosage at constant $FeCl_3$ dosage; (**c**,**d**) pH and $FeCl_3$ dosage at constant PSE dosage; (**e**,**f**) PSE dosage and $FeCl_3$ dosage at constant pH.

3.4.4. Phosphate Removal

As shown in Figure 8a,b, the interaction between PSE and pH plays a significant role in phosphate removal. At the central point of the parameters tested, the treated wastewater exhibited a reduction in phosphate concentration to 0.012 mg/L when using a chemical coagulant dosage of 5.5 mL/L. This behavior was mainly attributed to the deprotonation of functional groups in the PSE, which enhances the number of available adsorption sites, thereby improving phosphate removal efficiency.

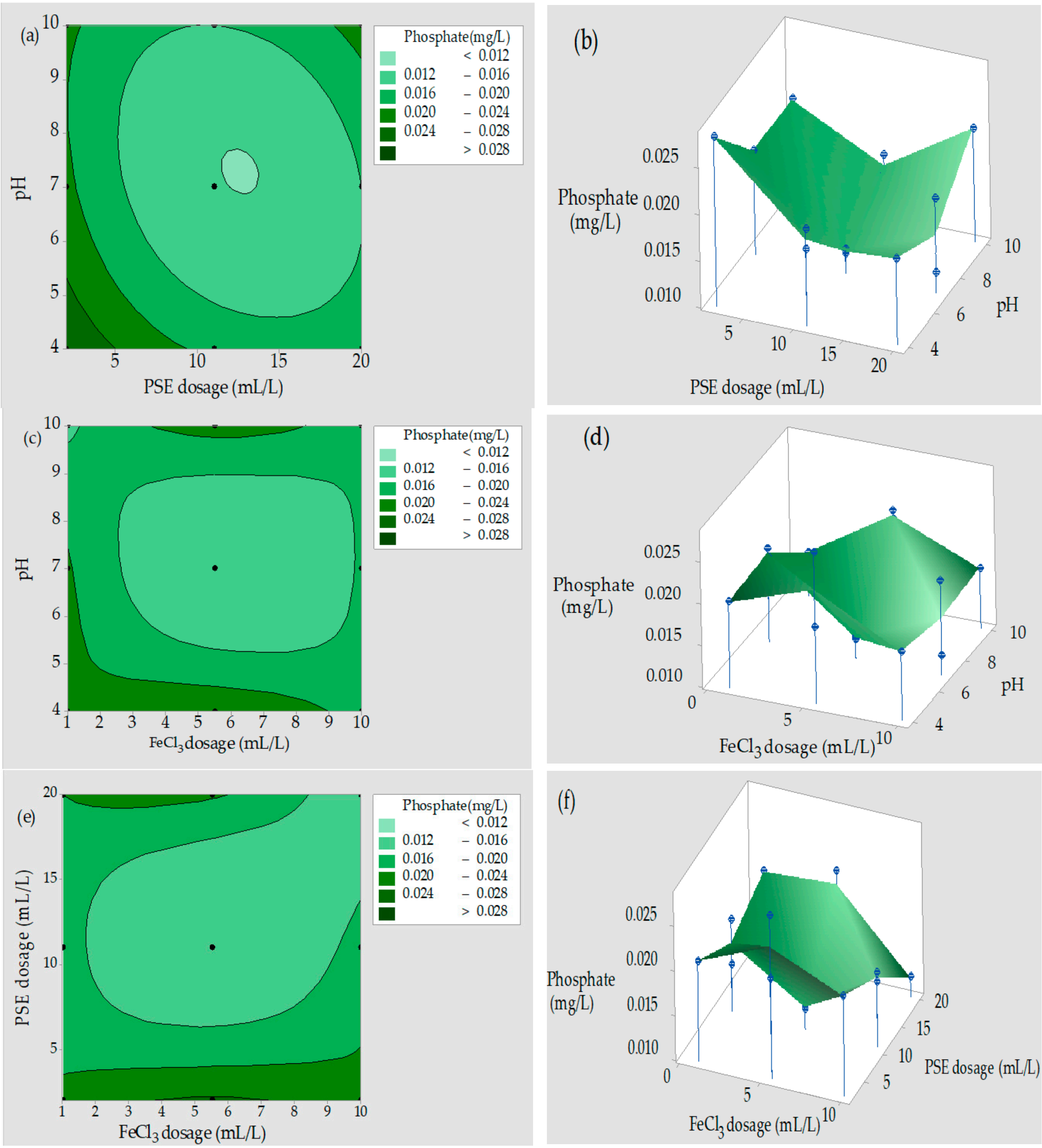

Figure 8. Contour plots and their corresponding surface plots for phosphate of wastewater as a function of (**a**,**b**) pH and PSE dosage at constant $FeCl_3$ dosage; (**c**,**d**) pH and $FeCl_3$ dosage at constant PSE dosage; (**e**,**f**) PSE dosage and $FeCl_3$ dosage at constant pH.

Figure 8c,d further demonstrates that the most effective phosphate reduction occurred at a neutral pH (7) with an optimal coagulant dosage ($FeCl_3$) of 5.5 mL/L, combined with 11 mL/L of PSE. However, at pH levels above 9, phosphate removal efficiency slightly declined due to competition between phosphate and hydroxide ions for adsorption sites. Additionally, at pH values exceeding 9, measurement biases may occur due to the high concentration of hydroxide ions (OH^-). Conversely, at an acidic pH of 4, phosphate removal dropped significantly to an unsatisfactory level. This reduction is likely due to the presence of hydronium ions (H_3O^+), which compete with phosphate ions for electrostatic interactions with the positively charged metal species, such as iron. As a result, the neutralization of negatively charged phosphate is hindered, reducing the overall coagulation efficiency.

The impact of the interaction between the chemical and bio-coagulants on phosphate removal at pH 7.0 is shown in Figure 8e,f. The results indicate that phosphate removal improves when both coagulants are used within a moderate dosage range. This suggests a positive interaction between the coagulants, enhancing the coagulation process. Furthermore, the statistical analysis (Equation (5)) confirms the significance of this interaction, reinforcing the reliability of the observed trend.

3.5. Analysis of Variance (ANOVA)

The statistical estimators R^2, adjusted R^2, and the *p*-value were used to evaluate the validity of the mathematical models. The results for turbidity, COD, phosphate, and UV 254 removal are presented in Table 3.

Table 3. R^2, R^2-adjusted and *p* values for each model.

	R^2	R^2 Adjusted	*p*
Phosphate (mg/L)	97.02%	91.65%	0.003
COD (mg/L)	98.41%	95.56%	0.001
Turbidity (NTU)	97.21%	92.18%	0.002
UV 254 (Cm^{-1})	98.62%	96.15%	0

The correlation coefficient (R^2) quantifies the relationship between the experimental data and the predicted responses [47]. A comparison between the experimental results and the model-predicted values (Equations (2)–(5)) showed a strong correlation, with R^2 values of 0.9721, 0.9841, 0.9702, and 0.9862 for turbidity removal, COD removal, phosphate removal, and UV 254 removal, respectively.

The adjusted R^2 also assesses the best fit but is more appropriate for comparing models with different numbers of independent variables. It accounts for the sample size and the number of terms in the model by incorporating degrees of freedom into its calculation. When a model includes many terms and the sample size is relatively small, Adj-R^2 may be noticeably lower than R^2 [47]. In this study, the adjusted R^2 values (0.9218, 0.9556, 0.9165, and 0.9615) for turbidity, COD, phosphate, and UV 254 removal were very close to the corresponding R^2 values, confirming the reliability of the models.

Additionally, *p*-values were used to determine the significance of each coefficient, which is essential for understanding the interactions between variables [47]. A *p*-value <0.05 signifies statistical significance, confirming the validity and acceptability of the quadratic model [47,48]. As shown in Table 3, all models had *p*-values below 0.005, confirming their significance.

3.6. Optimization

The objective of the optimization tool was to maximize the reduction in each parameter using the constraints shown in Table 4. The best results obtained are noted for a pH of 4, a PSE dosage of 17.8182 (mL/L), and a $FeCl_3$ dosage of 10 (mL/L).

Table 4. Optimal values.

Factor			Responses			
pH	PSE dosage (mL/L)	$FeCl_3$ dosage (mL/L)	Turbidity (NTU)	COD (mg/L)	UV 254 (cm^{-1})	Phosphate (mg/L)
4	17.8182	10	0.7546	190.882	0.00283	0.01487

3.7. Optimization and Model Validation of Experimental Parameters

After identifying the optimal coagulation conditions, the validation of the regression models was carried out through experiments conducted at this optimal point. The predicted values from the models were then compared with the experimental results, and the relative error was computed. Table 5 summarizes the outcomes for the removal of turbidity, COD, UV254, and phosphate.

Table 5. Physical and chemical characterization of water treated under optimal conditions.

Parameter	Unit	Raw Water	Y Predicted	Y Observed	Error
Turbidity	NTU	250	0.7546	0.77835	0.02375
COD	mg/L	640	190.882	194.382	3.5000
UV 254	cm^{-1}	0.893	0.00283	0.01385	0.01102
Phosphate	mg/L	0.115	0.01487	0.01538	0.00051

Table 5 presents a comparison between the experimental results and the values predicted by the mathematical models for turbidity, COD, UV254 absorbance, and phosphate residuals in treated wastewater. The close alignment between these values with differences remaining below 3.5 units demonstrates the reliability and robustness of the developed models. Moreover, all the investigated parameters showed significant reductions after treatment (see Figure 9), confirming the effectiveness of the natural coagulant (PSE) combined with the chemical coagulant ($FeCl_3$) under optimal conditions. The final values of the treated water meet acceptable discharge standards, indicating not only improved water quality but also compliance with environmental regulations. These results highlight the potential of the proposed treatment approach for practical application in wastewater management.

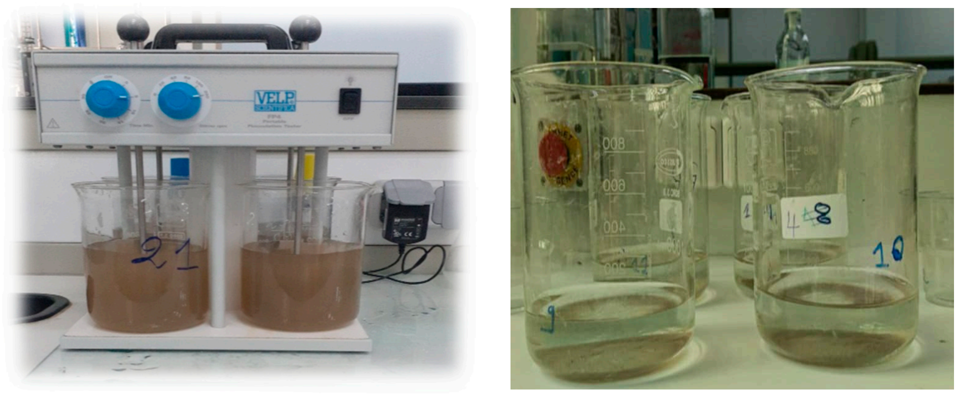

(**a**) (**b**)

Figure 9. Visual representation of wastewater: (**a**) before treatment; and (**b**) after treatment.

4. Conclusions

This work proposes an original study, as it will allow us, on one hand, to provide interesting contributions in the field of waste valorization after the extraction of essential oils. On the other hand, it will enable the possibility of introducing new natural product during the physicochemical treatment through the coagulation–flocculation process. The novelty of this work was the combination of a bio-coagulant based on *Pumpkin seed* waste and an iron-based chemical coagulant for wastewater treatment. The results obtained were highly significant: (i) the infrared spectrum showed the presence of several functional groups responsible for the coagulation–flocculation process, notably the carboxyl group (C=O) and NH amides; (ii) the experimental results allowed for the modeling and optimization of the coagulation–flocculation process in the wastewater treatment. In this case, all statistical indicators ($R^2 \geq 97\%$ and $p \leq 0.05$) confirm that the developed models are statistically validated for simulating the coagulation–flocculation process. Notably, the residual values of turbidity, COD, UV 254, and phosphate after treatment were 0.754 NTU, 190.88 mg/L, 0.0028 cm^{-1}, and 0.0149 mg/L, respectively. In this context, the corresponding values for pH, bio-coagulant dosage, and chemical coagulant dosage were 4, 17.81 mL/L, and 10 mL/L, respectively; (iii) this study opens up several prospects for research and sustainable development applicable to the treatment of pharmaceutical industrial waste using the coagulation–flocculation process, as well as for economic studies and the application of the combinations (PSE and $FeCl_3$) on an industrial scale. Finally, the possibility of using *Pumpkin* waste as a raw material for another treatment process, namely adsorption.

Author Contributions: Conceptualization, A.B., K.D., A.K. (Amel Khediri), N.F., O.B. and A.P.; methodology, A.B., N.F., K.E.Z., A.K. (Amel Khediri) and K.D.; formal analysis, O.B. and A.B.; investigation, A.B. and N.F.; data curation, A.B., K.E.Z., A.K. (Amel Khediri), K.D. and N.F.; writing—original draft preparation, A.B., O.B., K.E.Z., A.K. (Amel Khediri), K.D., N.F., A.K. (Amel Khalfaoui) and A.P.; writing—review and editing, A.B., O.B., K.D., A.K. (Amel Khalfaoui) and A.P.; supervision, K.D., A.K. (Amel Khalfaoui), A.B. and A.P.; project administration, A.B. and K.D. All authors have read and agreed to the published version of the manuscript.

Funding: This research received no external funding.

Institutional Review Board Statement: Not applicable.

Informed Consent Statement: Not applicable.

Data Availability Statement: The data that support the findings of this study are available on request from the corresponding author.

Acknowledgments: This work was supported by the École National Biotechnologie de Constantine (Algeria), Ecole Normale Supérieure de Constantine (Algeria) and Ecole National Polytechnique de Constantine (Algeria).

Conflicts of Interest: The authors declare that they have no conflicts of interest.

Abbreviations

PS	*Pumpkin seeds*
PSE	*Pumpkin seeds* extract
BBD	Box–Behnken design
COD	chemical oxygen demand
$FeCl_3$	Ferric chloride
FTIR	Fourier transform infrared spectrometer
HCl	dihydrogen chloride
NaCl	sodium chloride
NaOH	sodium hydroxide
RSM	response surface methodology
SEM	scanning electron microscope
UV 254	aromatic organic matter

References

1. Lemessa, F.; Simane, B.; Seyoum, A.; Gebresenbet, G. Assessment of the Impact of Industrial Wastewater on the Water Quality of Rivers around the Bole Lemi Industrial Park (BLIP), Ethiopia. *Sustainability* **2023**, *15*, 4290. [CrossRef]
2. Owhonka, A.; Fubara, E.F.; Justice, O.B. Wastewater Quality—It's Impact on the Environment and Human Physiology: A Review. *Int. J. Adv. Res. Innov.* **2021**, *9*, 43–58. [CrossRef]
3. Li, X.; Bao, L.; Wei, Y.; Zhao, W.; Wang, F.; Liu, X.; Su, H.; Zhang, R. Occurrence, Bioaccumulation, and Risk Assessment of Microplastics in the Aquatic Environment: A Review. *Water* **2023**, *15*, 1768. [CrossRef]
4. Hammami, S. Étude de Dégradation Des Colorants de Textile Par Les Procédés d'Oxydation Avancée. Application à La Dépollution Des Rejets Industriels. Ph.D. Thesis, Université de Marne la Vallée, Champs-sur-Marne, France, 2008.
5. Mansour, H.B.; Boughzala, O.; Barillier, D.; Mosrati, R. Les Colorants Textiles Sources de Contamination de l'eau: CRIBLAGE de La Toxicité et Des Méthodes de Traitement. *Rev. Sci. L'Eau* **2011**, *24*, 209–238. [CrossRef]
6. Kasperchik, V.P.; Yaskevich, A.L.; Bil'Dyukevich, A.V. Wastewater Treatment for Removal of Dyes by Coagulation and Membrane Processes. *Pet. Chem.* **2012**, *52*, 545–556. [CrossRef]
7. Yao, S.; Fabbricino, M.; Race, M.; Ferraro, A.; Pontoni, L.; Aimone, O.; Chen, Y. Study of the Digestate as an Innovative and Low-Cost Adsorbent for the Removal of Dyes in Wastewater. *Processes* **2020**, *8*, 852. [CrossRef]
8. Alardhi, S.M.; Albayati, T.M.; Alrubaye, J.M. A Hybrid Adsorption Membrane Process for Removal of Dye from Synthetic and Actual Wastewater. *Chem. Eng. Process.—Process Intensif.* **2020**, *157*, 108113. [CrossRef]
9. Zou, H.; Ma, W.; Wang, Y. A Novel Process of Dye Wastewater Treatment by Linking Advanced Chemical Oxidation with Biological Oxidation. *Arch. Environ. Prot.* **2015**, *41*, 33–39. [CrossRef]
10. Szpyrkowicz, L.; Juzzolino, C.; Kaul, S.N. A Comparative Study on Oxidation of Disperse Dyes by Electrochemical Process, Ozone, Hypochlorite and Fenton Reagent. *Water Res.* **2001**, *35*, 2129–2136. [CrossRef]
11. Zaharia, C.; Suteu, D.; Muresan, A.; Muresan, R.; Popescu, A. Textile Wastewater Treatment by Homogeneous Oxidation with Hydrogen Peroxide. *Environ. Eng. Manag. J.* **2009**, *8*, 1359–1369. [CrossRef]
12. Yildiz, B.S. Water and Wastewater Treatment: Biological Processes. In *Metropolitan Sustainability: Understanding and Improving the Urban Environment*; Woodhead Publishing Series in Energy; Woodhead Publishing: Sawston, UK, 2012; pp. 406–428. [CrossRef]
13. Chen, G.; Ekama, G.A.; van Loosdrecht, M.C.M.; Brdjanovic, D. *Biological Wastewater Treatment*; Taylor & Francis: London, UK, 2020; pp. 1–840. [CrossRef]
14. Exley, C. La Toxicité de l'aluminium Chez l'homme. *Morphologie* **2016**, *100*, 51–55. [CrossRef]
15. Rondeau, V.; Commenges, D.; Jacqmin-gadda, H.; Dartigues, J. Relation between Aluminum Concentrations in Drinking Water and Alzheimer's Disease: An 8-Year Follow-up Study. *Am. J. Epidemiol.* **2000**, *152*, 59–66. [CrossRef] [PubMed]
16. Zengjin, W.; Xiaomin, W.; Junlin, Y.; Jinning, S.; Jingyi, C.; Xianchen, L.; Zhao, X. Chronic Exposure to Aluminum and Risk of Alzheimer's Disease: A Meta-Analysis. *Neurosci. Lett.* **2016**, *610*, 200–206. [CrossRef]
17. Ndabigengesere, A.; Narasiah, K.S. Quality Of Water Treated By Coagulation Using Moringa Oleifera Seeds. *Water Res.* **1998**, *32*, 781–791. [CrossRef]
18. Megersa, M.; Beyene, A.; Ambelu, A.; Triest, L. Comparison of Purified and Crude Extracted Coagulants from Plant Species for Turbidity Removal. *Int. J. Environ. Sci. Technol.* **2019**, *16*, 2333–2342. [CrossRef]
19. Benalia, A. Extraction et Valorisation Des Produits Actifs Des Plantes Naturelles En Tant Que Bio Coagulants Utiles Dans L'amelioration de Qualite Des Eaux. Doctorat Thesis, University of Constantine 3, El Khroub, Algeria, 2023.
20. Benalia, A.; Derbal, K.; Amrouci, Z.; Baatache, O.; Khalfaoui, A.; Pizzi, A. Application of Plant-Based Coagulants and Their Mechanisms in Water Treatment: A Review. *J. Renew. Mater.* **2024**, *12*, 667–698. [CrossRef]
21. Prathna, T.C.; Srivastava, A. Ferric Chloride for Odour Control: Studies from Wastewater Treatment Plants in India. *Water Pract. Technol.* **2021**, *16*, 35–41. [CrossRef]
22. Poon, C.S.; Chu, C.W. The Use of Ferric Chloride and Anionic Polymer in the Chemically Assisted Primary Sedimentation Process. *Chemosphere* **1999**, *39*, 1573–1582. [CrossRef]
23. Dabhi, Y.M. Physicochemical Treatment of Dairy Plant Wastewater. *Int. J. Basic Appl. Chem. Sci.* **2013**, *3*, 9–14.
24. Rice, E.W.; Baird, R.B.; Eaton, A.D. (Eds.) *Standard Methods for the Examination of Water and Wastewater*, 22nd ed.; American Water Works Association (AWWA) and Water Environment Federation (WEF): Washington, DC, USA, 2012; ISBN 978-087553-0130.
25. Bouteflika, A. Valeurs Limites Des Paramètres de Rejets d'effluents Liquides Industriels. *J. Off. République Algérienne* **2006**, *26*, 1–27.
26. Box, G.E.P.; Behnken, D.W. Some New Three Level Designs for the Study of Quantitative Variables. *Technometrics* **1960**, *2*, 37–41. [CrossRef]
27. Almeida, M.; Erthal, R.; Padua, E.; Silveira, L.; Am, L. Talanta Response Surface Methodology (RSM) as a Tool for Optimization in Analytical Chemistry. *Talanta* **2008**, *76*, 965–977. [CrossRef]
28. Ouiem, B.; Kerroum, D.; Benalia, A.; Khalfaoui, A.; Pizzi, A. Optimization and Modeling of Bio-coagulation Using Pine Cone as a Natural Coagulant: Jar Test and Pilot-Scale Applications. *Water Air Soil Pollut.* **2024**, *235*, 770. [CrossRef]

29. Baatache, O.; Derbal, K.; Benalia, A.; Khalfaoui, A.; Bouchareb, R.; Panico, A.; Pizzi, A. Use of Pine Cone as Bio-Coagulant for Heavy Metal Removal from Industrial Wastewater: Use of Box—Behnken Design. *Ind. Crops Prod.* **2024**, *210*, 118185. [CrossRef]
30. Benalia, A.; Atime, L.; Baatache, O.; Khalfaoui, A.; Fadia, A. Removal of Lead in Water by Coagulation Flocculation Process Using Cactus—Based Natural Coagulant: Optimization and Modeling by Response Surface Methodology (RSM). *Environ. Monit. Assess.* **2024**, *196*, 244. [CrossRef]
31. Kebede, T.G.; Dube, S.; Mhuka, V.; Nindi, M.M. Bioremediation of Cd (II), Pb (II) and Cu (II) from Industrial Effluents by Moringa Stenopetala Seed Husk. *J. Environ. Sci. Health Part A* **2019**, *54*, 337–351. [CrossRef]
32. Dao, M.; Nguyen, V.; Tran, T.; Nguyen, X.; Vo, D.; Nguyen, V.; Hoang, L. Pilot-Scale Study of Real Domestic Textile Wastewater Treatment Using *Cassia fistula* Seed-Derived Coagulant. *J. Chem.* **2021**, *2021*, 7608856. [CrossRef]
33. Saritha, V.; Karnena, M.K.; Dwarapureddi, B.K. Competence of Blended Coagulants for Surface Water Treatment. *Appl. Water Sci.* **2020**, *10*, 20. [CrossRef]
34. Getahun, M.; Asaithambi, P.; Befekadu, A.; Alemayehu, E. Chemical Oxygen Demand Removal from Wet Coffee Processing Wastewater Using Indigenous Natural Coagulants: Optimization through Response Surface Methodology. *Desalination Water Treat.* **2024**, *317*, 100217. [CrossRef]
35. Desta, W.M.; Bote, M.E. Wastewater Treatment Using a Natural Coagulant (Moringa Oleifera Seeds): Optimization through Response Surface Methodology. *Heliyon* **2021**, *7*, e08451. [CrossRef]
36. Getahun, M.; Befekadu, A.; Alemayehu, E. Coagulation Process for the Removal of Color and Turbidity from Wet Coffee Processing Industry Wastewater Using Bio-Coagulant: Optimization through Central Composite Design. *Heliyon* **2024**, *10*, e27584. [CrossRef] [PubMed]
37. Benalia, A.; Derbal, K. Etude Expérimentale et Modélisation Du Processus de La Coagulation Floculation: Application Aux Eaux Destinée a La Consommation. Master's Thesis, University of Constantine 3, El Khroub, Algeria, 2015.
38. Bahrodin, M.B.; Zaidi, N.S.; Hussein, N.; Sillanpää, M.; Prasetyo, D.D.; Syafiuddin, A. Recent Advances on Coagulation-Based Treatment of Wastewater: Transition from Chemical to Natural Coagulant. *Curr. Pollut. Rep.* **2021**, *7*, 379–391. [CrossRef]
39. Nguyen, H.T.; Luc, T.Q.; Hoang, H.V.; Cao, H.T.; Tran, L.P.T. Treatment Surface Water Using a Novel Pumpkin Seed-Based Natural Bio-Coagulant: Optimization by CCD and Toxicity Evaluation. *Glob. Nest J.* **2023**, *25*, 142–148. [CrossRef]
40. Baptista, A.T.A.; Silva, M.O.; Gomes, R.G.; Bergamasco, R.; Vieira, M.F.; Vieira, A.M.S. Protein Fractionation of Seeds of Moringa Oleifera Lam and Its Application in Superficial Water Treatment. *Sep. Purif. Technol.* **2017**, *180*, 114–124. [CrossRef]
41. Ebrahimi, A.; Amin, M.M.; Hajizadeh, Y.; Pourzamani, H.; Memarzadeh, M.; Mahvi, A.H.; Mahdavi, M. Filter Backwash Water Treatment by Coagulation: A Comparison Study by Polyaluminium Ferric Chloride and Ferric Chloride. *Desalination Water Treat.* **2017**, *66*, 320–329. [CrossRef]
42. Muniz, G.L.; da Silva, T.C.F.; Borges, A.C. Assessment and Optimization of the Use of a Novel Natural Coagulant (Guazuma Ulmifolia) for Dairy Wastewater Treatment. *Sci. Total Environ.* **2020**, *744*, 140864. [CrossRef]
43. Gohari Ardabili, A.; Farhoosh, R.; Haddad Khodaparast, M.H. Chemical Composition and Physicochemical Properties of Pumpkin Seeds (Cucurbita Pepo Subsp. Pepo Var. Styriaka) Grown in Iran. *J. Agric. Sci. Technol.* **2011**, *13*, 1053–1063.
44. Abidin, Z.Z.; Ismail, N.; Yunus, R.; Ahamad, I.S.; Idris, A. A Preliminary Study on Jatropha Curcas as Coagulant in Wastewater Treatment. *Environ. Technol.* **2011**, *32*, 971–977. [CrossRef]
45. Al-gheethi, A.; Mohamed, R.; Wurochekke, A.; Nurulainee, N.; Mas Rahayu, J.; Amir Hashim, M. Efficiency of Moringa Oleifera Seeds for Treatment of Laundry Wastewater. *MATEC Web Conf.* **2017**, *103*, 1–8. [CrossRef]
46. Otálora, M.C.; Wilches-Torres, A.; Lara, C.R.; Gómez Castaño, J.A.; Cifuentes, G.R. Evaluation of Turbidity and Color Removal in Water Treatment: A Comparative Study between Opuntia Ficus-Indica Fruit Peel Mucilage and FeCl3. *Polymers* **2023**, *15*, 217. [CrossRef]
47. Khataee, A.R.; Zarei, M.; Fathinia, M.; Jafari, M.K. Photocatalytic Degradation of an Anthraquinone Dye on Immobilized TiO_2 Nanoparticles in a Rectangular Reactor: Destruction Pathway and Response Surface Approach. *Desalination* **2011**, *268*, 126–133. [CrossRef]
48. Sibiya, N.P.; Amo-Duodu, G.; Tetteh, E.K.; Rathilal, S. Model Prediction of Coagulation by Magnetised Rice Starch for Wastewater Treatment Using Response Surface Methodology (RSM) with Artificial Neural Network (ANN). *Sci. Afr.* **2022**, *17*, e01282. [CrossRef]